Out of balance: implications of climate change for the ecological stoichiometry of harmful cyanobacteria

van de Waal, D.B.

Chapter 3

The ecological stoichiometry of toxins produced by harmful cyanobacteria: an experimental test of the carbon-nutrient balance hypothesis

ABSTRACT - The elemental composition of primary producers reflects the availability of light, carbon, and nutrients in their environment. According to the carbon-nutrient balance hypothesis, this has implications for the production of secondary metabolites. To test this hypothesis, we investigated a family of toxins, known as microcystins, produced by harmful cyanobacteria. The strain *Microcystis aeruginosa* HUB 5-2-4, which produces several microcystin variants of different N:C stoichiometry, was cultured in chemostats supplied with various combinations of nitrate and CO_2. Excess supply of both nitrogen and carbon yielded high cellular N:C ratios accompanied by high cellular contents of total microcystin and the nitrogen-rich variant microcystin-RR. Comparable patterns were found in *Microcystis*-dominated lakes, where the relative microcystin-RR content increased with the seston N:C ratio. In total, our results are largely consistent with the carbon-nutrient balance hypothesis, and warn that a combination of rising CO_2 and nitrogen enrichment will affect the microcystin composition of harmful cyanobacteria.

This chapter is based on the paper: Dedmer B Van de Waal, Jolanda MH Verspagen, Miquel Lürling, Ellen Van Donk, Petra M Visser, and Jef Huisman. 2009. The ecological stoichiometry of toxins produced by harmful cyanobacteria: an experimental test of the carbon-nutrient balance hypothesis. Ecology Letters 12: 1326-1335.

3.1 Introduction

Primary producers link the living with the nonliving world through the conversion of light energy, CO_2 and inorganic nutrients into biomass. The relative availability of these inorganic resources is a major determinant of the elemental stoichiometry of primary producers, and affects their production of organic compounds such as fatty acids, proteins and nucleic acids (Sterner and Elser 2002; Klausmeier *et al*. 2004; Moe *et al*. 2005). The relative availability of carbon and nutrients may also affect the production of secondary metabolites, which often play a role as toxins in anti-herbivore defence. For instance, according to the carbon-nutrient balance hypothesis (Bryant *et al.* 1983; see also Stamp 2003), nutrient limitation will favour carbon-based metabolites such as phenols, whereas nitrogen-rich metabolites such as alkaloids are favoured in fertile ecosystems. Eutrophication and the global rise of atmospheric CO_2 concentrations are currently enriching many ecosystems with vast loads of carbon and nutrients. This could alter the carbon-nutrient balance of primary producers (Van de Waal *et al*. 2010) and their production of secondary metabolites (Bezemer and Jones 1998; Reich *et al*. 2006).

Harmful cyanobacteria are notorious toxin producers, which proliferate in many eutrophic waters (Reynolds 1987; Huisman *et al*. 2005). During weak vertical wind mixing, buoyant cyanobacteria float to the water surface (Walsby *et al*. 1997; Huisman *et al*. 2004; Jöhnk *et al*. 2008). Accumulation of cyanobacterial cells at the water surface leads to the formation of dense surface blooms. High toxin concentrations in dense surface blooms pose a major threat to birds, mammals and human health, and make the water less suitable for drinking water, agricultural irrigation, fishing, and recreational use (Chorus and Bartram 1999; Carmichael 2001; Paerl and Huisman 2008). Dense cyanobacterial blooms can strip surface waters from dissolved inorganic carbon, depleting the carbon availability for photosynthesis to limiting levels (Ibelings and Maberly 1998). However, the current rise in atmospheric CO_2 concentrations (Solomon *et al*. 2007) may counter this process by enriching surface waters with carbon dioxide, and could thereby shift dense surface blooms from carbon limitation to nutrient and/or light limitation.

Several harmful cyanobacteria produce a family of toxins known as microcystins. Microcystins are nonribosomal peptides that may cause serious damage to the liver (Sivonen and Jones 1999; Carmichael 2001; Huisman *et al*. 2005). Nitrogen is an important constituent of microcystins, and nitrogen availability is known to affect the microcystin production of isolated strains (Long *et al*. 2001; Downing *et al*. 2005). Microcystins consist of seven amino acids, including two positions with a variable amino acid composition. At present, at least 89 different microcystin variants have been described (Welker and Von Döhren 2006). The composition of microcystin variants differs among cyanobacterial strains, and also depends on the intracellular availability of different amino acids that can occupy the variable positions (Tonk *et al*. 2008). Common microcystin variants include microcystin-LR, microcystin-RR, and microcystin-YR. These three variants are identical

except at the first variable amino acid position, which is occupied by leucine (L), arginine (R) or tyrosine (Y), respectively (Sivonen and Jones 1999; Hesse and Kohl 2001). The amount of nitrogen in these amino acids differs. Arginine contains four nitrogen atoms while leucine and tyrosine each contain only one nitrogen atom. As a consequence, the molar N:C ratio of microcystin-RR (N:C = 0.27) is higher than that of microcystin-LR and microcystin-YR (N:C = 0.20 and N:C = 0.19, respectively). Hence, could enhanced nitrogen loading and rising CO_2 levels affect the carbon to nutrient stoichiometry of harmful cyanobacteria? And, if so, could this affect their production and composition of microcystins?

In this paper, we test the hypothesis that changes in the relative availability of nitrogen and carbon dioxide will affect the cellular N:C stoichiometry, total microcystin content, and microcystin composition of cyanobacteria. To investigate this hypothesis, we have grown the freshwater cyanobacterium *Microcystis aeruginosa* HUB 5-2-4 in chemostats at different concentrations of dissolved inorganic nitrogen and CO_2. In addition, we also analyzed the microcystin composition and seston stoichiometry of several *Microcystis*-dominated lakes to investigate whether our laboratory findings are consistent with lake observations. Our results show that an increase in nitrogen availability can shift the microcystin composition towards the nitrogen-richest variant microcystin-RR. Moreover, our results demonstrate that the toxin composition of harmful cyanobacteria is especially affected by rising CO_2 concentrations in nitrogen-rich waters, which may present a likely future scenario for many eutrophic lakes.

3.2 Materials and methods

Experimental set-up - The cyanobacterium *Microcystis aeruginosa* HUB 5-2-4 was provided by the Humboldt University of Berlin, Germany. The predominant microcystin variants produced by this strain are microcystin-LR, microcystin-RR, and microcystin-YR (Hesse and Kohl 2001). This *Microcystis* strain was cultured as single cells in laboratory chemostats with flat culture vessels specifically designed for phytoplankton studies (Matthijs *et al.* 1996; Huisman *et al.* 2002). The chemostat cultures were unialgal but not axenic. Regular microscopic inspection confirmed that population densities of heterotrophic bacteria remained low (i.e., well below 1% of the total biomass). The chemostats had an optical path length ('mixing depth') of 5 cm, and a working volume of 1.7 L. They were maintained at a constant temperature of 23 ± 1 ºC using a metal cooling finger connected to a Colora thermocryostat, and at a constant incident irradiance (I_{in}) of 50 ± 1 µmol photons m^{-2} s^{-1} supplied by white fluorescent tubes (Philips PL-L 24W/840/4P; Philips Lighting). The chemostats were aerated with sterilised (0.2 µm Millex-FG Vent Filter, Millipore) and moistened N_2 gas enriched with different CO_2 concentrations to a final gas flow of 25 L hr^{-1} using Brooks Mass Flow Controllers (Brooks Instrument).

Previous studies have found a strong correlation between cellular microcystin contents and the growth rate of *Microcystis* (Orr and Jones 1998; Long *et al*. 2001). To avoid confounding effects of differences in growth rate, we therefore ran all our experiments at the same dilution rate of 0.15 d^{-1}. At steady state, the specific growth rate of *Microcystis* will equal the dilution rate of the chemostat, and hence the specific growth rate will be the same in all experiments irrespective of the imposed experimental treatment. The mineral medium consisted of different concentrations of $NaNO_3$ (Table 3.1), 220 µM K_2HPO_4, 400 µM $MgSO_4$, 180 µM $CaCl_2$, 500 µM $NaHCO_3$, 22 µM $FeCl_2$, 14 µM Na_2EDTA, 44 µM H_3BO_3, 9 µM $MnCl_2$, 0.8 µM $ZnSO_4$, 0.0016 µM $(NH_4)6Mo_7O_{24}$, 0.3 µM $CuSO_4$ and 0.3 µM $Co(NO_3)_2$.

Experimental treatments - Ten chemostats were supplied with different concentrations of $NaNO_3$ in the mineral medium and different concentrations of CO_2 in the gas flow (Table 3.1). Nitrate concentrations in our mineral medium were one or two orders of magnitude higher than the nitrate concentrations typically found in eutrophic lakes. This might suggest that the applicability of our chemostat experiments is limited. Under light-limited conditions, however, phytoplankton population density scales inversely with mixed-layer depth (Huisman 1999; Diehl *et al*. 2002). More specifically, a given light supply per unit area can support a given primary production per unit area. This primary production, which is typically distributed over several meters depth in lakes, is now compressed into our chemostats of only 5 cm depth. This scaling rule results in very high population densities in light-limited laboratory chemostats (Huisman *et al*. 2002). To sustain these high population densities, while avoiding nitrogen limitation, requires mineral media with high nitrogen concentrations. Similarly, the high primary production of laboratory chemostats also requires a sufficient supply of CO_2. This was achieved by a high gas flow rate through our chemostats, such that we could maintain the CO_2 concentrations within the natural range. Dissolved CO_2 concentrations may vary from < 10 ppm in lakes with dense phytoplankton blooms (Maberly 1996) to > 5000 ppm in lakes with high concentrations of dissolved organic carbon (Sobek *et al*. 2005).

We expected that chemostats supplied with low $NaNO_3$ concentrations will become nitrogen limited, chemostats supplied with low CO_2 concentrations will become carbon limited, while chemostats supplied with high inputs of both $NaNO_3$ and CO_2 will become light limited. The limiting resource was assessed post-hoc, by measurements of the residual concentrations of nitrate and dissolved inorganic carbon, the phycocyanin to chlorophyll-a ratio, pH, and light penetration through the chemostat vessels (I_{out}). The pigment phycocyanin is a nitrogen-rich compound that is very sensitive to nitrogen availability (Allen 1984), and hence can be used as a good indicator of nitrogen limitation. Depletion of CO_2 leads to a high pH, which can be used as a good indicator of carbon

Table 3.1. Overview of the experimental treatments and steady-state characteristics. Depending on the concentration of $NaNO_3$ in the mineral medium and CO_2 in the gas flow, the chemostats became either nitrogen-, carbon-, or light-limited. Superscript letters indicate significant differences between the steady-state characteristics of these three different resource limitations (based on one-way ANOVA and post-hoc comparison of the means).

Chemostat	Treatment			Steady-state characteristics						
	$NaNO_3$ (µM)	CO_2 (ppm)	Limitation	Residual nitrate (µM)	PC:Chl-a ratio*	DIC_{av} (µM)†	pH	I_{out} (µmol m^{-2} s^{-1})‡	Population density ($\times 10^9$ cells L^{-1})	Cell diameter (µm)
1	200	400	N	3.4^a	0.13^a	1133^a	7.7^a	20.3^a	10.2^a	3.9^a
2	200	800	N	1.2^a	0.11^a	745^a	7.5^a	17.3^a	11.5^a	4.0^a
3	400	100	N	4.5^a	0.10^a	902^a	9.2^a	17.9^a	12.9^a	3.6^a
4	400	800	N	8.0^a	0.11^a	1952^a	8.4^a	19.3^a	13.1^a	3.5^a
5	400	50	C	75.8^b	0.18^b	688^b	10.0^b	20.4^a	2.6^b	4.5^b
6	12000	50	C	9355^b	0.20^b	212^b	10.7^b	15.9^a	4.5^b	4.4^b
7	12000	100	C	9236^b	0.25^b	318^b	10.7^b	9.9^a	6.9^b	4.5^b
8	12000	400	Light	8852^b	0.31^c	2512^a	8.5^a	4.8^b	13.3^a	4.3^{ab}
9	12000	2800	Light	9567^b	0.30^c	2172^a	7.5^a	5.6^b	16.6^a	4.0^{ab}
10	12000	2800	Light	8191^b	0.36^c	4168^a	8.5^a	3.5^b	21.7^a	3.9^{ab}

** PC:Chl-a ratio = phycocyanin to chlorophyll-a ratio.*

† DIC_{av} = dissolved inorganic carbon available for photosynthesis (sum of dissolved carbon dioxide and bicarbonate).

‡ I_{out} = light penetration through the chemostat vessel

limitation in our experiments. Depletion of the light flux through the chemostat vessels (i.e., a low I_{out}) is indicative of light limitation (Huisman 1999; Huisman *et al.* 2002).

Measurements - At steady state, the chemostats were sampled and several variables were measured every other day for a period of ten days. The incident irradiance (I_{in}) and the irradiance penetrating through the chemostat vessel (I_{out}) were measured with a LI-COR LI-250 quantum photometer (LI-COR Biosciences) at 10 randomly chosen positions on the front and back surface of the chemostat vessel, respectively. The pH was measured with a SCHOTT pH meter (SCHOTT AG). Absorbances of chlorophyll-a (chl-a) and phycocyanin (PC) were measured in culture suspensions at wavelengths of 438 nm and 627 nm, respectively, using an Aminco DW-2000 double-beam spectrophotometer (SLM Instruments Inc.). Biovolumes and cell concentrations were determined in triplicate using a Casy 1 TTC cell counter with a 60 µm capillary (Schärfe System GmbH).

Intracellular C and N content were sampled in triplicate. Samples were pressurized at 10 bar to collapse the gas vesicles of *Microcystis* and subsequently centrifuged for 15 min at 2000 *g*. After discarding the supernatant, the pellet was resuspended in demineralised water, and centrifuged for 5 min at 15 000 *g*. The supernatant was discarded, pellets were stored at 20 ºC and subsequently freeze dried and weighed to determine dry weight. The C and N content of homogenised freeze-dried cell powder was analysed using a Vario EL Elemental Analyzer (Elementar Analysensysteme GmbH).

Residual nitrate concentrations and dissolved inorganic carbon concentrations in the chemostats were determined by sampling 15 mL of culture suspension, which was immediately filtered over 0.45 µm membrane filters (Whatman). Nitrate concentrations were analyzed using a Skalar SA 400 autoanalyzer (Skalar Analytical). The dissolved inorganic carbon concentration (DIC) was analyzed by a Model 700 TOC Analyzer (OI Corporation). Cyanobacteria use carbon dioxide and bicarbonate for carbon fixation, but not the carbonate ion. We therefore define available DIC (DIC_{av}) as the sum of the carbon dioxide and bicarbonate concentration, which was calculated from total DIC and pH (Stumm and Morgan 1996).

Intracellular microcystin contents were determined in triplicate by sampling 5-20 mL of culture suspension, which was immediately filtered using Whatman GF/C filters (pore size ~1.2 µm). Filters were frozen at -20 °C and subsequently freeze-dried. Microcystins were extracted in three rounds with 75% MeOH according to Fastner *et al*. (1998), with an additional step for grinding of the filters using a Mini Beadbeater (BioSpec Products) with 0.5 mm silica beads (Tonk *et al*. 2005). Dried extracts were stored at -20 °C and dissolved in 50% MeOH for microcystin analysis using high performance liquid chromatography (HPLC) with photodiode array detection (Kontron Instruments, Watford, UK). The different microcystin variants were separated using a LiChrospher 100 ODS 5 µm LiChorCART 250-4 cartridge system (Merck) and a 30 to 70% acetonitrile gradient in milli-Q water with 0.05% trifluoroacetic acid at a flow rate of 1 mL min^{-1}. Identification of

the different microcystin variants was based on their characteristic UV-spectra (Lawton *et al*. 1994), and quantified using gravimetrical standards of microcystin-LR, microcystin-RR (both provided by the University of Dundee) and microcystin-YR (Sigma-Aldrich). Since *Microcystis* changed its cell size in response to the experimental treatments (Table 3.1), we expressed intracellular microcystin contents per unit of cellular biovolume. Extracellular microcystin concentrations were considered negligible, as they always comprised less than 3% of the total microcystin concentrations in the chemostat experiments.

Lake survey - In August 2007, 19 water samples were collected from 12 freshwater lakes in The Netherlands in which the phytoplankton community was dominated by *Microcystis* spp. (see Table A1 in Appendix 1). From each lake, 10 L was sampled from ~1 m depth during the late morning. Additionally, we also took samples near the water surface (at ~5 cm depth) in those lakes that showed dense surface blooms. Microcystin concentrations and seston C and N contents were analyzed as described above. *Microcystis* abundances were quantified by inverted light microscopy, after disintegration of the colonies into single cells according to Kardinaal *et al.* (2007a).

Statistical analysis - In total, we obtained time series of 5 consecutive steady-state measurements for each chemostat experiment. These were time-averaged, to obtain a single value of each measured variable in each chemostat. Based on these data, we clustered the ten chemostat experiments into three groups (nitrogen limited, carbon limited, light limited). Significant differences between the three groups were tested using one-way ANOVA, followed by post-hoc comparison of the means using Tukey's HSD (Sokal and Rohlf 1995). Variables were log-transformed if this improved the homogeneity of variances, as evaluated by Levene's test.
The experimental data suggested that the relationships between microcystin contents and cellular N:C ratio were nonlinear. We investigated these relationships by fitting the data to a three-parameter exponential model:

$$y = y_0 + a\mathrm{e}^{bx} \tag{3.1}$$

where x is the cellular N:C ratio, y is the cellular microcystin content, and y_0 can be interpreted as the 'baseline' microcystin content. This is a nonlinear model, because the baseline y_0 prevents transformation of the model to a linear form. Parameter estimation was based on minimization of the residual sum of squares using the iterative procedure of nonlinear regression (SPSS version 16.0). Parameter estimates were validated by checking convergence of the iteration for different initial conditions. We tested the three-parameter model of Eq. 3.1 against a two-parameter exponential model without baseline microcystin

content using Schwarz's (1978) Bayesian Information Criterion (BIC). In all cases, this showed that the three-parameter model gave the "better fit" (i.e., a lower BIC value).

Lake data were analyzed by testing for associations between the cellular microcystin content and N:C ratio of lake seston. Because the cellular microcystin content and relative microcystin-RR content of lake seston were not normally distributed (as evaluated by the Shapiro-Wilk test), the associations were investigated using Spearman's rank correlation test (Sokal and Rohlf 1995).

3.3 Results

Resource limitation - All chemostat experiments reached a steady state within ~40 days. The steady-state characteristics enabled clustering of the chemostat experiments into three groups according to their resource limitation (Table 3.1). At steady state, nitrogen-limited chemostats had significantly lower residual nitrate concentrations (ANOVA on log-transformed nitrate data, $F_{2,7}$ = 25.3, P = 0.001) and phycocyanin:chlorophyll-a ratios (ANOVA, $F_{2,7}$ = 60.1, P < 0.001) than carbon-limited and light-limited chemostats. Carbon-limited chemostats had significantly lower population densities (ANOVA, $F_{2,7}$ = 16.5, P = 0.002), significantly lower concentrations of available DIC (ANOVA on log-transformed DIC_{av} data, $F_{2,7}$ = 15.3, P = 0.003) and significantly higher pH (ANOVA, $F_{2,7}$ = 13.8, P = 0.004) than nitrogen-limited and light-limited chemostats. Light-limited chemostats had high concentrations of residual nitrate and available DIC but significantly lower light penetration through the chemostat vessels (ANOVA, $F_{2,7}$ = 19.6, P = 0.001) than nitrogen-limited and carbon-limited chemostats. Cell diameter also varied between the treatments. Cells in carbon-limited chemostats were significantly larger (ANOVA, $F_{2,7}$ = 12.9, P = 0.005) than cells in nitrogen-limited chemostats, while the cells in light-limited chemostats were of intermediate size (Table 3.1).

N:C stoichiometry - The cellular N:C ratio varied between treatments, and increased with the ratio of dissolved inorganic nitrogen to available DIC in the chemostat vessel (Fig. 3.1a; linear regression: R^2 = 0.82, n = 10, P < 0.001). Differences in cellular N:C ratio were not reflected in the cellular carbon content (Fig. 3.1b; linear regression: R^2 = 0.05, n = 10, P = 0.55). As a consequence, there was a strong relationship between the cellular nitrogen content and the N:C ratio of the cells (Fig. 3.1c; linear regression: R^2 = 0.97, n = 10, P < 0.0001).

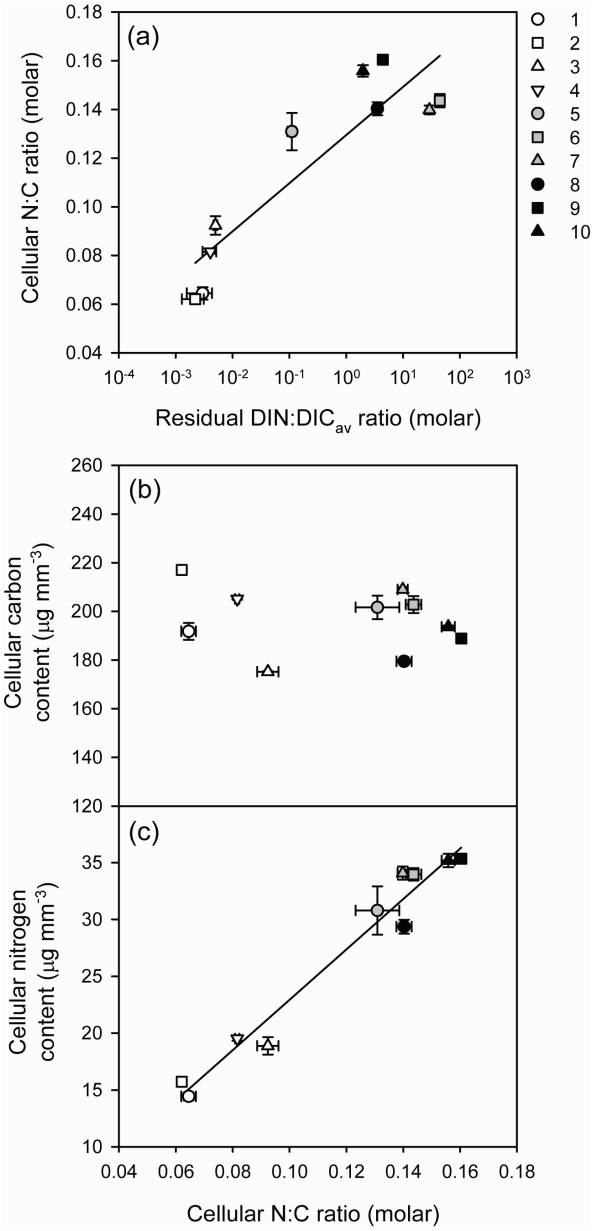

Figure 3.1. (a) Cellular N:C ratio as a function of the ratio of dissolved inorganic nitrogen to available dissolved inorganic carbon (DIN:DIC$_{av}$ ratio) in the chemostat vessel. (b) Cellular carbon content and (c) cellular nitrogen content in relation to the cellular N:C ratio. Each data point represents a steady-state chemostat, grown under nitrogen limitation (white symbols), carbon limitation (grey symbols), or light limitation (black symbols). Error bars indicate the standard error of the mean (n = 5). Numbers correspond to the chemostats enlisted in Table 3.1. Significant regressions are shown by solid lines.

Microcystin composition - Microcystin-LR and microcystin-RR were the predominant microcystin variants in the chemostat experiments, together accounting for more than 80% of the total cellular microcystin in all treatments. The microcystin-LR content did not change over the measured range of cellular N:C ratios (Fig. 3.2a; nonlinear regression: y_0 = 0.31 µg mm^{-3}, R^2 = 0.01). In contrast, both microcystin-RR and microcystin-YR increased with the cellular N:C ratio (Fig. 3.2b,c; nonlinear regression for microcystin-RR: y_0 = 0.060 µg mm^{-3}, R^2 = 0.90; nonlinear regression for microcystin-YR: y_0 = 0.062 µg mm^{-3}, R^2 = 0.66). This pattern is reflected in the total cellular microcystin content, which also increased with the cellular N:C ratio (Fig. 3.2d; nonlinear regression: y_0 = 0.43 µg mm^{-3}, R^2 = 0.62). The relative contribution of microcystin-RR to the total cellular microcystin content increased with the cellular N:C ratio (Fig. 3.3c; nonlinear regression: y_0 = 13.28, R^2 = 0.81).

Lake survey - Microcystin concentrations in the sampled lakes varied over more than three orders of magnitude, and were strongly related to *Microcystis* abundance (Fig. 3.3a; linear regression: R^2 = 0.85, n = 19, P < 0.001). The cellular microcystin content did not correlate with the seston N:C ratio (Fig. 3.3b; Spearman's rank correlation: ρ = -0.126, n = 19, P = 0.303). In many lakes, microcystin-LR was the most abundant microcystin variant, and in some lakes it was even the only microcystin variant that could be detected (Appendix 1). Microcystin-RR and microcystin-YR were found in many lakes as well, ranging from 0 to ~50% of the total microcystin concentration in the lake seston. Other microcystin variants always contributed less than 5% of the total microcystin concentration. The lake samples showed a remarkably similar range in relative microcystin-RR contents and seston N:C ratios as the chemostat experiments (Fig. 3.3c). More specifically, the relative microcystin-RR content in the lakes showed a significant positive correlation with the seston N:C ratio when all lake samples were included in the analysis (Spearman's rank correlation: ρ = 0.557, n = 19, P = 0.007). When lake samples without microcystin-RR were excluded, the positive correlation was on the edge of significance (Spearman's rank correlation: ρ = 0.418, n = 16, P = 0.054). The three lake samples without microcystin-RR all had low seston N:C ratios (Fig. 3.3c).

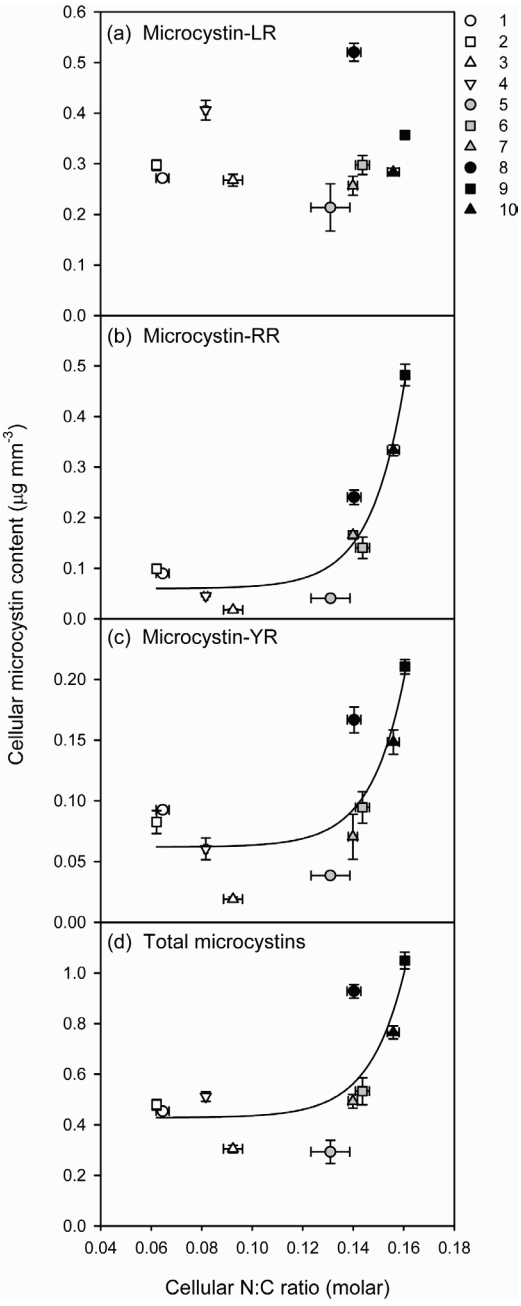

Figure 3.2. Cellular contents of (a) microcystin-LR, (b) microcystin-RR, (c) microcystin-YR, and (d) total microcystins in relation to the cellular N:C ratio. Each data point represents a steady-state chemostat, grown under nitrogen limitation (white symbols), carbon limitation (grey symbols), or light limitation (black symbols). Error bars indicate the standard error of the mean (n = 5). Numbers correspond to the chemostats enlisted in Table 3.1. Solid lines show the fit of the three-parameter exponential model.

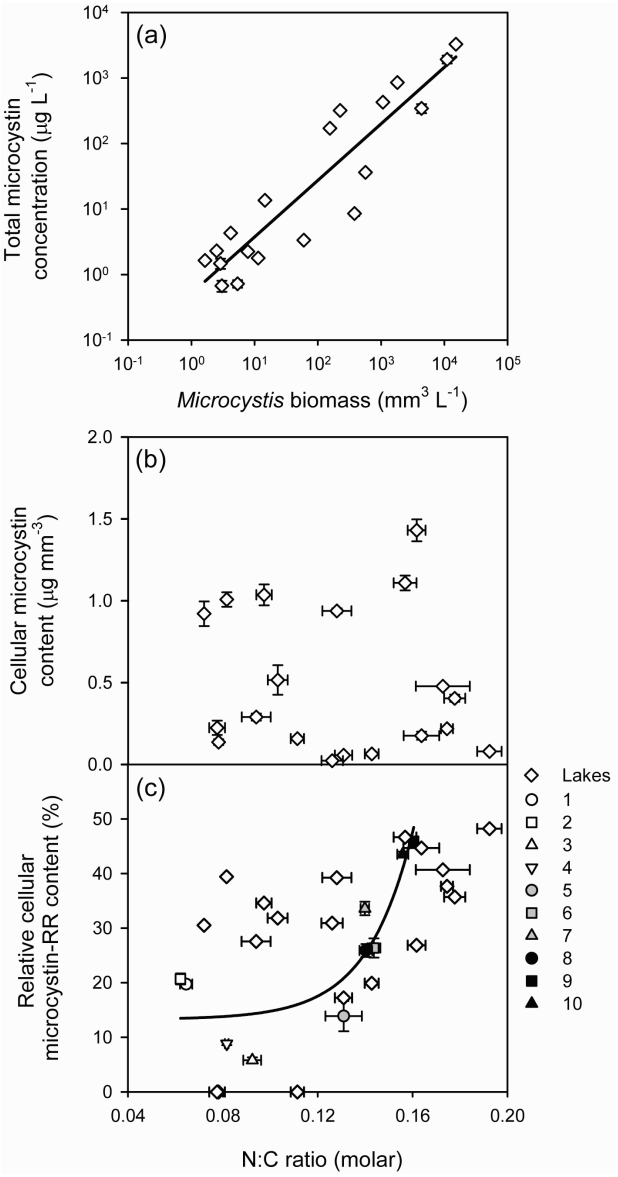

Figure 3.3. (a) Total microcystin concentration in several lakes as a function of *Microcystis* biomass. Each data point represents a different lake sample. The solid line is based on linear regression. (b) The cellular microcystin content of *Microcystis* in relation to the seston N:C ratio measured in the lake samples. (c) Relative contribution of microcystin-RR to the total microcystin content plotted as a function of the N:C ratio. Data points in (c) represent lake samples (open diamonds) as well as steady-state chemostat experiments (other symbols). The solid line shows the fit of the three-parameter exponential model to the chemostat data. The chemostats were grown under nitrogen limitation (white symbols), carbon limitation (grey symbols), or light limitation (black symbols). Numbers correspond to the chemostats enlisted in Table 3.1. Error bars indicate the standard error of the mean (n = 3 for the lake data, n = 5 for the chemostat experiments). The lake data are tabulated in Table A1 of Appendix 1.

3.4 Discussion

Our results show that the environmental availability of inorganic nitrogen and inorganic carbon affects the cellular N:C stoichiometry and microcystin composition of harmful cyanobacteria. The amount of nitrogen invested in microcystins was only a small fraction, less than 1%, of the total amount of nitrogen in the cells. Yet, the total microcystin content varied 4-fold across the experimental treatments, consistent with earlier studies that showed a similar range of variation (Long *et al.* 2001; Wiedner *et al*. 2003; Kardinaal and Visser 2005b). The microcystin composition responded even stronger. In particular, the cellular content of the variant microcystin-RR showed a 50-fold variation across the different chemostat experiments. Apparently, environmental growth conditions have a much larger impact on the production of individual microcystin variants than on the total microcystin production.

To what extent are our results consistent with the carbon-nutrient balance hypothesis (Bryant *et al.* 1983; Stamp 2003) and the more general theory of ecological stoichiometry (Sterner and Elser 2002)? The carbon-nutrient balance hypothesis inspired much research comparing carbon-based versus nitrogen-based secondary metabolites of primary producers, but also sparked a heated debate (Hamilton *et al*. 2001; Koricheva 2002; Stamp 2003). For instance, it has been pointed out that nitrogen-rich alkaloids are produced by a different enzymatic machinery, and may be even more costly in terms of carbon investments than many carbon-based phenols (Hamilton *et al*. 2001). In other words, it was argued that studies comparing the carbon-nutrient stoichiometry of different secondary metabolites compared apples with oranges. In our study, we could circumvent this important criticism on the carbon-nutrient balance hypothesis. Microcystins constitute a family of closely related toxins that are all synthesized nonribosomally by the same enzymatic machinery (Tillett *et al*. 2000; Welker and Von Döhren 2006). This large enzyme complex can incorporate a variety of different amino acids in the microcystin molecule, thus producing microcystin variants of different carbon-nutrient stoichiometry (Tonk *et al*. 2008).

Our results show that the microcystin composition of *Microcystis aeruginosa* is indeed sensitive to the availability of nitrogen and carbon. According to the carbon-nutrient balance hypothesis, one would expect a strong response of the nitrogen-rich variant microcystin-RR to changes in nitrogen and carbon availability. However, one would expect a less clear response, or perhaps no response at all, of microcystin variants that contain less nitrogen. As expected, at low nitrogen availability, cells were characterized by low cellular N:C ratios accompanied by low contents of the nitrogen-rich variant microcystin-RR (Fig. 3.2b). Conversely, excess supply of both nitrogen and carbon resulted in light-limited conditions with high cellular N:C ratios and high contents of microcystin-RR. Microcystin production seems to involve a fixed and a flexible component. The model fits indicate a fixed baseline production of each microcystin variant. On top of this baseline, cells produce

additional microcystin-YR and microcystin-RR at high nitrogen and carbon availability (Fig. 3.2). This combination of a fixed plus flexible component in microcystin production is in good agreement with the carbon-nutrient balance hypothesis, which predicts that the surplus of nitrogen and carbon is allocated to secondary metabolites (Stamp 2003). Interpretation of the microcystin composition in terms of nitrogen and carbon availability also offers a plausible explanation for earlier results of Tonk *et al.* (2005), who studied the microcystin composition of the filamentous cyanobacterium *Planktothrix agardhii* in relation to light availability. High light intensities enhance photosynthesis, which typically lead to low cellular N:C ratios (Sterner and Elser 2002). Indeed, the nitrogen-rich microcystin-RR variant decreased twofold, whereas the less nitrogen-rich microcystin-LR variant increased threefold with increasing light intensity (Tonk *et al*. 2005). All in all, these findings show that the carbon-nutrient balance hypothesis offers a suitable explanation for differences in microcystin composition under nitrogen-limited versus light-limited conditions.

Interestingly, however, we obtained different results under carbon-limited conditions. Carbon limitation yielded high intracellular N:C ratios, but not an increased microcystin-YR and microcystin-RR content (Fig. 3.2). The pronounced difference in microcystin production between carbon-limited and light-limited conditions was not predicted by the carbon-nutrient balance hypothesis. These observations might be explained by the coupling between nitrogen and carbon metabolism of cyanobacteria. For instance, it is known that nitrogen uptake rates of cyanobacteria are partly suppressed under carbon limitation (Tandeau de Marsac *et al*. 2001; Forchhammer 2004). This will restrict the intracellular availability of nitrogen for microcystin production under carbon-limited conditions. In contrast, both inorganic nitrogen and carbon are in excess under light-limited conditions, and their accumulation in the cells may enhance the production of microcystins. It is also known that several amino acids, including the amino acid arginine incorporated in microcystin-RR, can serve as a source of both nitrogen and carbon (Lu 2006; Commichau *et al.* 2006). Under carbon-limited conditions, cells might therefore utilize arginine as a carbon source and restrict the availability of this amino acid for microcystin-RR synthesis. Further research on the regulation of microcystin production will be needed to fully address this intriguing contrast between carbon-limited versus light-limited conditions.

To investigate whether the laboratory results would be consistent with lake observations, we measured concentrations of different microcystin variants in *Microcystis*-dominated lakes. This revealed that differences in *Microcystis* abundance caused substantial variation in the total microcystin concentrations in these lakes, consistent with findings of earlier studies (e.g., Kardinaal *et al*. 2007a). Whereas our chemostat experiments used only a single *Microcystis* strain, lakes often contain a mixture of different *Microcystis* genotypes producing different microcystin variants (Kardinaal *et al*. 2007a; Briand *et al*. 2009). Indeed, as anticipated, the relation between microcystin composition and seston N:C ratio was less clear in the lakes than in the chemostat experiments. Yet, the relative microcystin-

RR contents and N:C ratios in the lake samples spanned a similar range as in the chemostat experiments. Moreover, the lake samples showed a positive correlation between the relative microcystin-RR content and seston N:C ratio (Fig. 3.3c). These patterns indicate that, in essence, the lake data on the microcystin composition are consistent with our laboratory findings.

Microcystins are toxic for many invertebrates, birds, and mammals, including humans (Chorus and Bartram 1999; Carmichael 2001; Huisman *et al*. 2005). However, individual microcystin variants differ in their toxicity (Sivonen and Jones 1999). The toxicity of microcystins for mammals has been estimated by LD_{50} assays on mice. A lower LD_{50} value (the dose lethal for 50% of the mouse population) indicates a higher toxicity. In our experiment, microcystin-LR is the most toxic microcystin variant (LD_{50} = 50 µg kg^{-1}), closely followed by microcystin-YR (LD_{50} = 70 µg kg^{-1}), while microcystin-RR is the least toxic for mice (LD_{50} = 600 µg kg^{-1}; Sivonen and Jones 1999). We found that the cellular content of microcystin-LR was not affected by the treatments, while the cellular contents of microcystin-YR and microcystin-RR were highest under light-limited conditions. However, given that microcystin-RR is much less toxic than the other two microcystin variants, the marked increase in microcystin-RR content under light-limited conditions will probably yield only a small increase in the total toxicity of *Microcystis* cells.

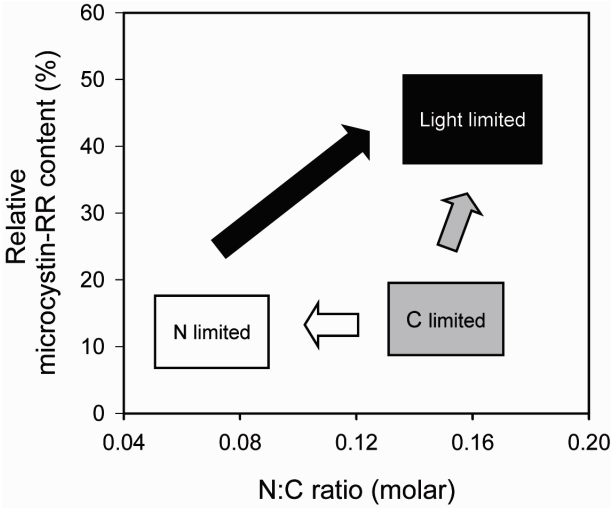

Figure 3.4 Schematic diagram of the relative microcystin-RR content and cellular N:C ratio, under nitrogen-, carbon- and light-limited conditions. Arrows indicate the predicted effects of rising CO_2 levels. The white arrow shows that a shift from carbon to nitrogen limitation will reduce the cellular N:C ratio, but will hardly affect the cellular microcystin composition. The grey arrow shows that a shift from carbon to light limitation will hardly affect the cellular N:C ratio, but will shift the microcystin composition towards microcystin-RR. The black arrow shows that a shift from nitrogen to light limitation, in waters enriched with nitrogen and CO_2, will increase both the cellular N:C ratio and cellular microcystin-RR content.

Several studies report that rising levels of atmospheric CO_2 increase the intracellular carbon to nitrogen ratio of phytoplankton and terrestrial plants (Reich *et al*. 2006; Urabe and Waki 2009; Van de Waal *et al.* 2010). According to our study, the impact of rising CO_2 on the carbon-nitrogen stoichiometry and microcystin composition of *Microcystis* will depend on the limiting resource (Fig. 3.4). Rising atmospheric CO_2 concentrations may alleviate dense surface blooms of *Microcystis* from carbon limitation (Ibelings and Maberly 1998). In nitrogen-poor waters, elevated CO_2 may therefore shift cyanobacterial blooms from carbon limitation towards nitrogen limitation. Our results show that this shift will reduce the N:C ratio of cyanobacterial cells, but has relatively little effect on their microcystin composition (Fig. 3.4). In contrast, in nitrogen-rich waters, elevated CO_2 will induce light-limited conditions. This will shift the microcystin composition of cells to higher concentrations of the nitrogen-rich variant microcystin-RR (Fig. 3.4). Thus, our findings warn that rising levels of atmospheric CO_2 in eutrophic waters will not only tend to favor cyanobacterial growth, but will also affect the ecological stoichiometry of the toxins they produce.

Acknowledgements - We thank Hans CP Matthijs for stimulating discussions and technical advice, and the anonymous reviewers for their valuable comments on the manuscript. The research of DBvdW, JH and PMV was supported by the Earth and Life Sciences Foundation (ALW) and the work of JMHV was supported by the NWO program Water, both subsidized by the Netherlands Organization for Scientific Research (NWO).